



*Supplement of*

## **Significant additional Antarctic warming in atmospheric bias-corrected ARPEGE projections with respect to control run**

**Julien Beaumet et al.**

*Correspondence to:* Julien Beaumet ([julien.beaumet@univ-grenoble-alpes.fr](mailto:julien.beaumet@univ-grenoble-alpes.fr))

The copyright of individual parts of the supplement might differ from the article licence.

## **S1 Method**

### **S1.1 ARPEGE model set-up**

In this section, further information are given on ARPEGE model set-up used in this study. The model is used with a T255 truncation configuration, a stretched Pole at 80°S, 90°E and a 2.5 stretching factor. This yields a grid point spacing ranging  
5 between 30 to 35 kms over most of East Antarctic to 45 to 50 kms over the northern part of the Antarctic Peninsula (Fig. S1a). Model surface height can also be seen in Fig. S1b. Differences between ARPEGE and MAR RCM Antarctic configuration at 35 kms horizontal resolution for model surface height can be seen in Fig. S2. Differences are small (< 200 m) over most of the Antarctic continent and are unlikely to explain most of temperature and precipitation differences evidenced in the different result section of the paper (section 3.1). However, more substantial differences in surface elevation (> 400 m) are found over  
10 the northern part of the Antarctic Peninsula, the Transantarctic mountains, and around the Amery Ice Shelf.

### **S1.2 Correction Term**

Some examples of the correction terms obtained are given in Fig. S3 for temperature and specific humidity at ~500 hPa (units are K and kg/kg respectively). Following Eq.1, the value of the correction applied on tendencies at each time step is obtained by multiplying these correction terms by  $\frac{\Delta t}{\tau}$ , with  $\Delta t=900s$  and  $\tau=72h$  in our simulation. Which gives for temperatures at ~500  
15 hPa an applied correction on tendencies equal to 0.0015 K/day for median of absolute values and of 0.0037 K/day for maximum of absolute values. The order of values of these terms are to be compared with typical values of tendencies from the model's physics: for instance typical values of tendencies associated with radiative (shortwave and longwave) heating rates of 0.5 to 2.5 K/day are found in Cesana et al. (2019). Since they are equivalent just to a few percent of the tendencies associated with the model physics, correction terms are unlikely to degrade significantly physical processes represent in the model. Nevertheless,  
20 as they are applied at each time step, the correction terms applied are sufficient to correct for most of the model biases on large-scale atmospheric circulation.

## **S2 Large-scale atmospheric circulation**

In this section, we present some of the results mentioned in the results or discussion section for large-scale atmospheric circulation in order to facilitate the comprehension of the discussion. In Fig. S4, we can see the large bias-reduction with respect to ERA-I for 200 hPa temperatures in ARP-AMIP-AC. However, we can see the slight increase in spring and winter of  
25 the warm bias over the South Pole already present in spring for AMIP.

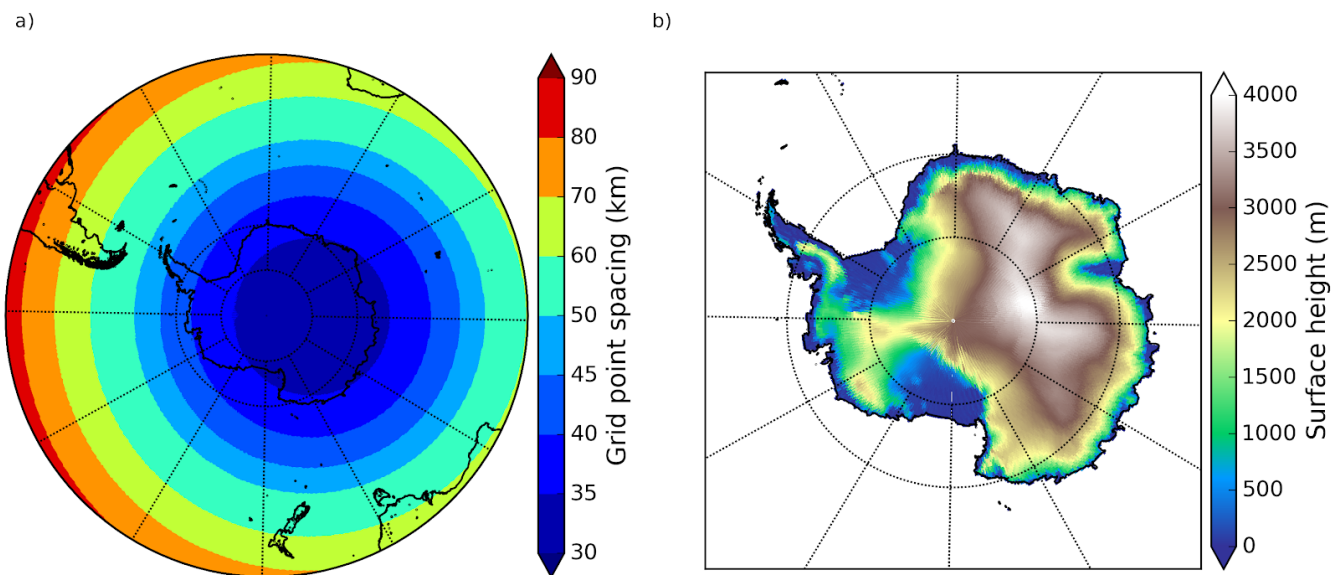


**Figure S1.** ARPEGE T255 truncation with stretching pole over East Antarctic ( $80^{\circ}\text{S}$ ,  $90^{\circ}\text{E}$ ) and stretching factor 2.5 grid point spacing (in kms, left) and model surface height (in m, right).

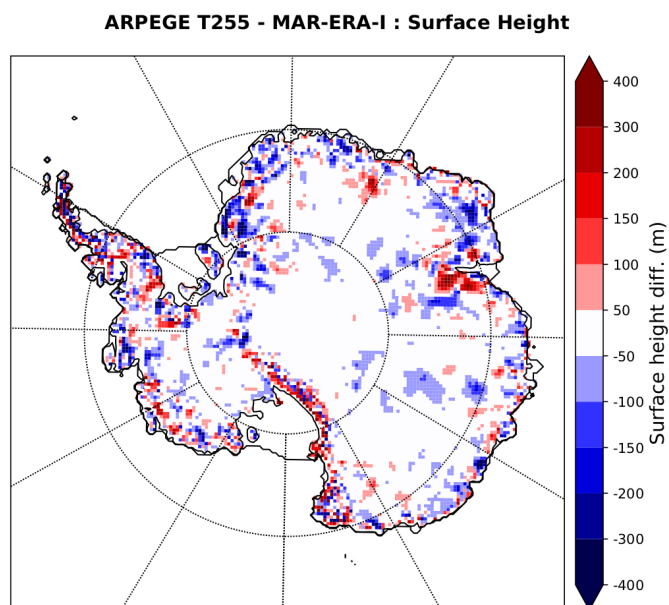


**Figure S2.** ARPEGE T255 with Antarctic zoom : surface height difference (in m) with MAR RCM at 35 kms horizontal resolution over Antarctica.

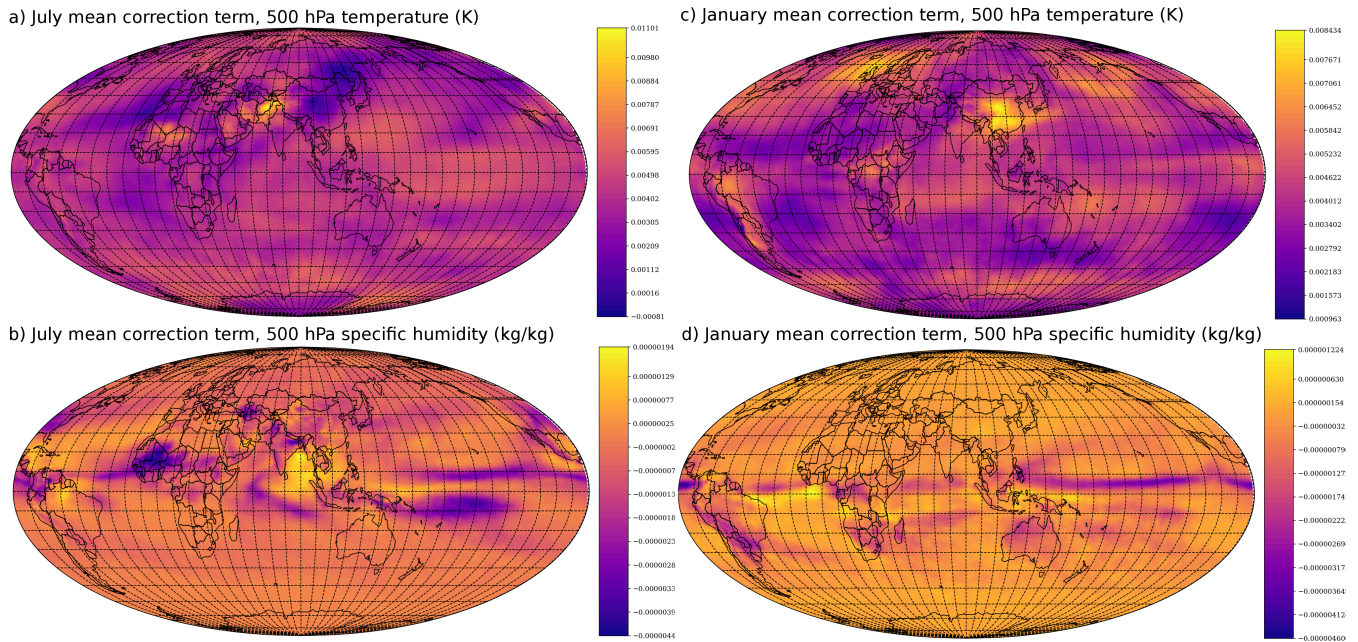


**Figure S3.** July mean correction term used in ARPEGE bias corrected experimented for air temperature (a) and specific humidity (c) at level 64 ( 500 hPa). Units are Kelvin and kg/kg respectively. (c) and (d), same as (a) and (b) but for January.

**Table S1.** Relative seasonal root mean square error reduction  $\Delta_r E$  (in %) south of  $20^\circ\text{S}$  with respect to ERA-Interim for ARP-AMIP-AC with respect to ARP-AMIP during the 1981-1992 period for different surface and tropospheric variables at constant pressure levels :

<i>Simulations</i>	JJA	SON	DJF	MAM
<b>SLP</b>	78	55	48	68
<b>T500</b>	91	93	94	89
<b>Z500</b>	87	83	72	81
<b>Q500</b>	3	1	77	-1

In Fig. S5, we can see the remaining bias on 850 hPa temperatures in ARP-AMIP-AC with respect to ERA-I. The bias is close to zero in most places except for relatively small warm bias ( $\sim 1\text{-}2\text{K}$ ) over mid-latitudes land masses (South America, South Africa and Australia). Wet or dry biases are found over the same places in 850 and 500 hPa specific humidity, but their sign vary depending on the season or the level considered (*figures not shown*). These biases were absent in ARP-AMIP (*figures not shown*) and probably results from errors on planetary boundary layer or clouds processes (i.e. convection).

In Fig. S6, we can see that there is substantial warming in winter 500 hPa temperatures in ARP-AMIP-AC with respect to AMIP. This warming resulted in an increase downward longwave radiation over the East Antarctic Plateau and explains the increase of the winter warm bias in this area in near-surface temperatures in ARP-AMIP-AC.

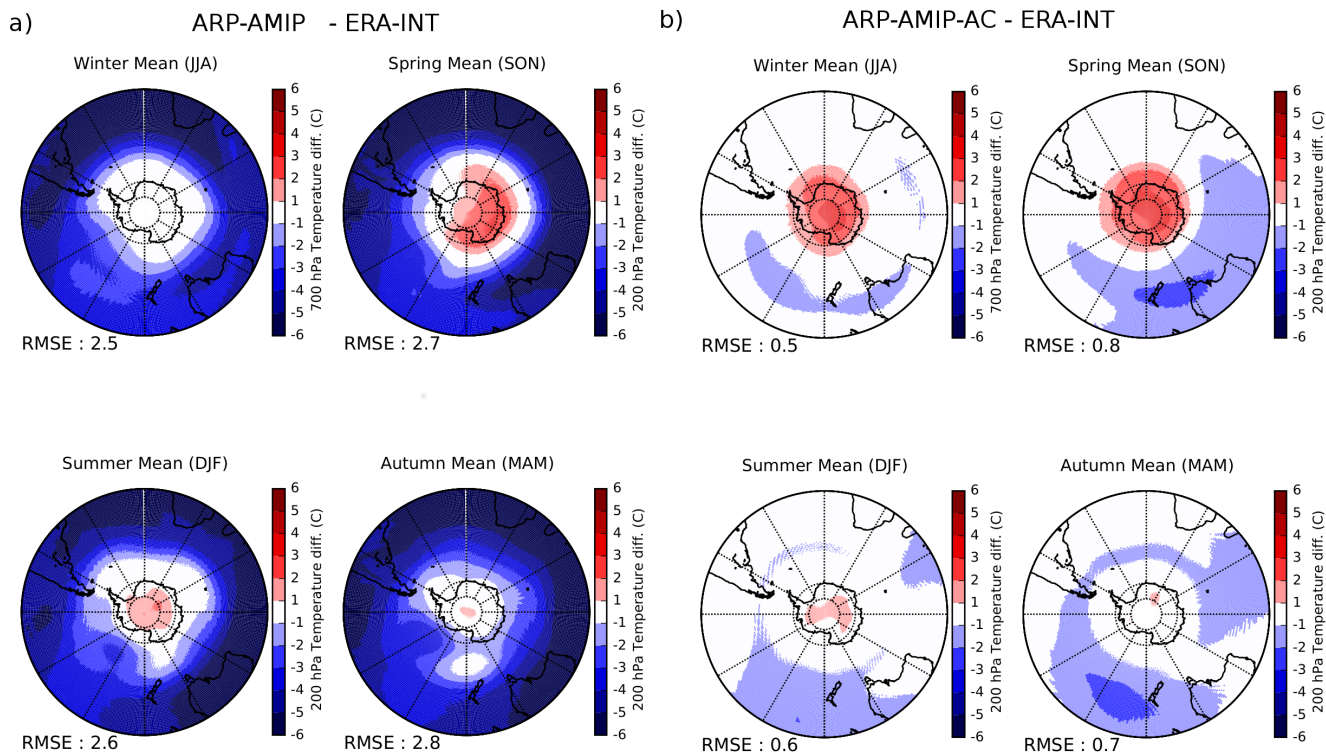


**Figure S4.** Seasonal ARP-AMIP (a) and ARP-AMIP-AC (b) error on 200 hPa temperature (K) with respect to ERA-Interim over 1981-2010.

### S3 CMIP5 ensemble comparison and link with previous studies

In this section, we put in the context of the coupled models large ensemble (CMIP5) the differences in projected changes in atmospheric general circulation between ARPEGE bias-corrected and non-corrected control projections. We focus on the main aspect of the projected change in large-scale atmospheric circulation in southern hemisphere, that is the poleward shift of the westerly winds maximum or eddy-driven jet (Arblaster and Meehl, 2006; Bracegirdle et al., 2013, 2018). Bracegirdle et al. (2013) evidenced a dependence between the position of the eddy-driven jet in climate model's historical simulation and the magnitude of the projected shift for the late 21<sup>st</sup> century : i.e models with more equator-ward biases on the position of the westerlies maximum (WMPOS) display a larger poleward shift in their future projection. In fig. S7, we represent this relationship for climate models of the CMIP5 ensemble and add the ARPEGE future projection presented in this study. Uncorrected ARPEGE projections show a northward bias on WJPOS larger than the CMIP5 ensemble mean and suggest a 21st century shift that falls within the values of projected changes for CMIP5 models that bear similar biases. Conversely, ARPEGE bias-corrected run shows very few bias on WMPOS and suggests a 21st century shift that also agree with the range of projected changes for CMIP5 models that agree with currently observed WMPOS in their historical simulation. Bracegirdle et al. (2013) mentioned the results of Barnes and Hartmann (2012) as possible physical processes for explaining these results : these authors

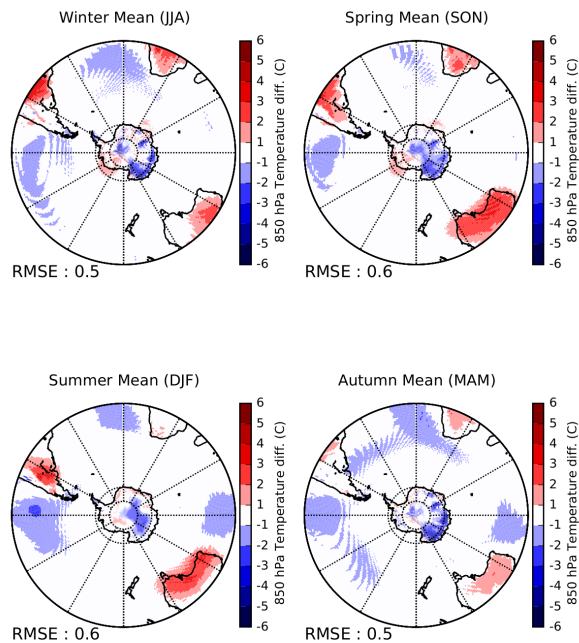


**Figure S5.** Seasonal ARP-AMIP-AC bias on 850 hPa temperatures with respect to ERA-I over 1981-2010.

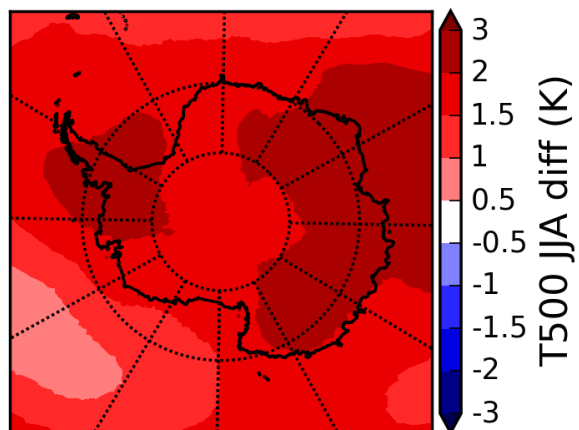


**Figure S6.** ARP-AMIP-AC - ARP-AMIP winter (JJA) 500 hPa temperatures

**Table S2.** Tropical (0 to 25°S, 250 hPa) and Polar (75 to 90°S, 150 hPa) stratospheric warming for ARPEGE projections. Change in gradient is defined as the projected change (future projection minus historical reference) in Tropical minus Polar stratospheric temperatures such as done in (Bracegirdle et al., 2013).

Simulations	Tropical (K)	Polar (K)	Gradient change (K)
ARP-NOR-21-OC	+4.9	+0.0	+5.0
ARP-NOR-21-AOC	+5.0	+1.0	+4.0
ARP-MIR-21-OC	+7.6	-1.0	+8.6
ARP-MIR-21-AOC	+7.4	+0.6	+6.8

**Table S3.** Distance between the subpolar eddy-driven jet and the sub-tropical jet for zonal mean, Atlantic (290°-20°), Pacific (150°-290°) and Indian Ocean (20°-150°) sector. Position of subpolar jet is taken as the maximum of zonal wind speed at 850 hPa, while the limit of the subtropical jet corresponds to the limit of 10 m.s<sup>-1</sup> on the equatorward side of the jet for zonal wind speed at 400 hPa following the work of (Simpson et al., 2012; Bracegirdle et al., 2013).

Simulations	Zonal	Atlantic	Pacific	Indian
ARP-AMIP	27.4	21.7	32.6	27.0
ARP-AMIP-AC	31.1	27.2	35.0	26.9

showed, using GCMs future projection and a barotropic model, that the cyclonic wave breaking on the poleward side of the jet is constrained by the meridional gradient of absolute vorticity and that there is theoretical limit to how far south cyclonic wave breaking will migrate under the influence of climate warming. These authors also suggested that currently observed climate is already close to this limit. These arguments all suggest that the projected change in the eddy-driven jet is expected to be much more realistic in ARPEGE bias-corrected projections than it is in non-corrected experiment.

Similarly to what has been done in (Bracegirdle et al., 2013) for models of the CMIP5 ensemble, we have also investigated in our ARPEGE simulations the polar stratospheric and equatorial upper-tropospheric warming as well as the changes in Tropical-Polar gradient following the work of Wilcox et al. (2012). Finally, the distances between the subpolar eddy-driven jet and the subtropical critical line (PT distance), similarly to what has been done in Simpson et al. (2012), have been computed for the zonal mean and for the different oceanic basin for ARP-AMIP and ARP-AMIP-AC. Consistent with previous studies, we found that the increase in the Tropical-Polar gradient of the upper atmosphere is lower, while the PT distance is higher in the bias-corrected experiments. These two mechanism have been linked with reduced poleward shift of the eddy-driven jet in Wilcox et al. (2012) and Simpson et al. (2012) respectively.

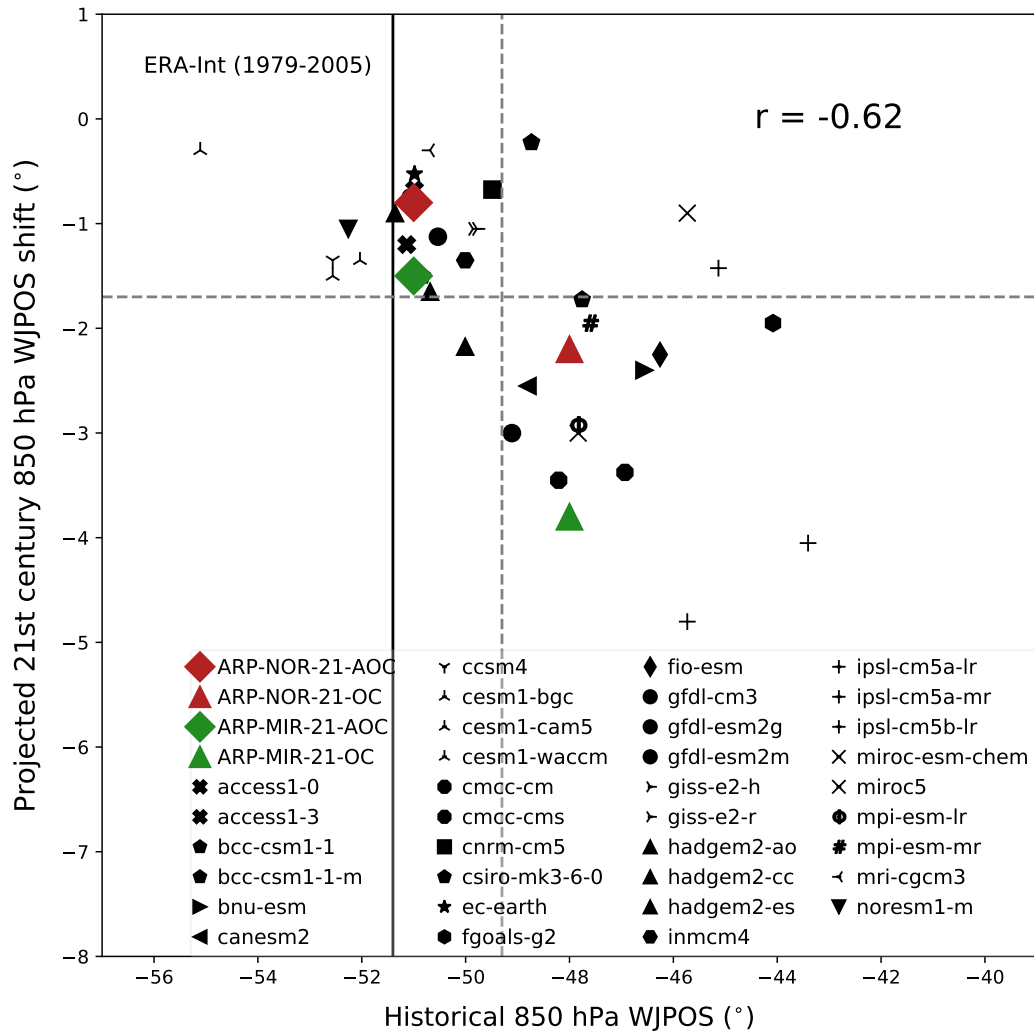


**Figure S7.** Late 21st century (2071-2100) projected (RCP8.5 scenario) in shift in 850 hPa westerly wind maximum position (WMPOS) as function of the position in the historical simulation (1979-2005, or 1981-2010 for ARPEGE simulations). Position of WMPOS in ERA-Interim reanalysis is shown (black vertical line) as well as CMIP5 ensemble mean (dashed lines).

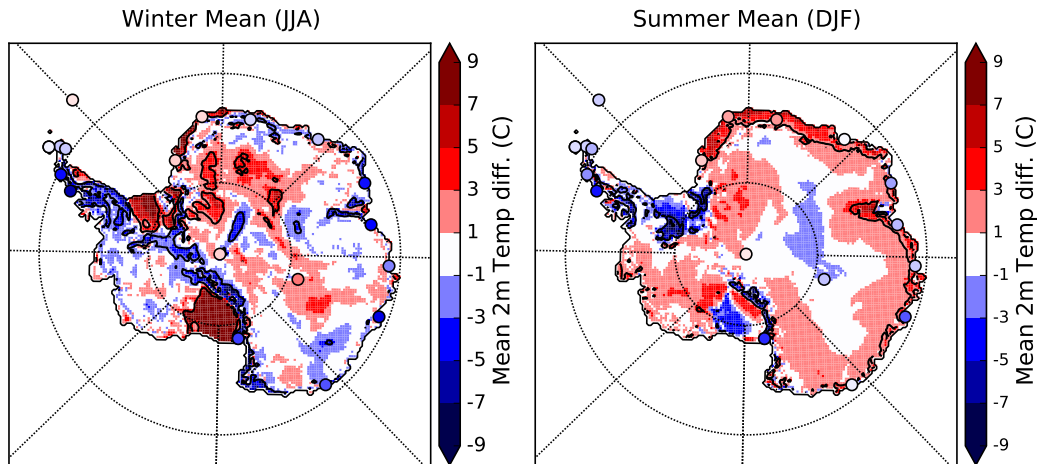


**Figure S8.** ARP-AMIP minus MAR-ERA-I  $T_{2m}$  in winter (*left*) and summer (*right*). Circles represent differences with stations from the monthly READER data base. *Black contour line* represents where the difference is one standard deviation of MAR  $T_{2m}$ .

#### S4 Near-Surface Temperatures

In this section, we present the difference with ERA-I driven MAR simulation in  $T_{2m}$  for the ARP-AMIP simulation (Fig. S8, already shown in Beaumet et al. (2019)). The differences with *in-situ* stations from READER data base are presented in Table S4 for ARP-AMIP-AC and ARP-AMIP. Mean bias for each Antarctic regions are also shown.

#### 5 S5 Surface Mass Balance

In this section, we present the comparison between ARP-AMIP-AC, ARP-AMIP, MAR ERA-I and RACMO2-ERA-I for surface sublimation (Fig. S9). Surface sublimation is significantly reduced in ARP-AMIP-AC with respect to ARP-AMIP and the agreement (RMSE) with the two polar-oriented RCMs is substantially reduced. However, surface sublimation at the continental scale is still widely overestimated in ARP-AMIP-AC owing to the excess of turbulent mixing near the surface  
 10 and to the dry biases in part due to unaccounted blowing snow sublimation, which is relevant in the comparison with RACMPO2.

**Table S4.** Error on READER weather station  $T_{2m}$  in the ARP-AMIP-AC (left) and ARP-AMIP (right) simulation for the reference period 1981-2010. Significant errors ( $p < 0.05$ ) are presented in **bold**. For each station, elevation difference (in m) between the corresponding ARPEGE grid point and the station elevation are shown in parenthesis. These differences have been accounted for in the comparison by correcting the model temperature using a dry adiabatic lapse rate of  $-0.9 \text{ K} \cdot 100 \text{ m}^{-1}$ .

Stations	DJF	MAM	JJA	SON	DJF	MAM	JJA	SON
<b>EAP</b>	<b>ARP-AMIP-AC</b>				<b>ARP-AMIP</b>			
Amundsen Scott (-44)	0.76	<b>3.15</b>	1.22	0.7	0.47	<b>2.4</b>	1.06	0.94
Vostok (-22)	<b>-1.12</b>	<b>4.45</b>	<b>5.44</b>	<b>2.24</b>	<b>-1.46</b>	<b>3.21</b>	<b>3.22</b>	<b>1.89</b>
<i>Mean error</i>	-0.18	3.80	3.33	1.47	-0.50	2.81	2.14	1.42
<b>Coastal EA</b>	<b>ARP-AMIP-AC</b>				<b>ARP-AMIP</b>			
Casey (+27)	<b>-0.94</b>	<b>-3.5</b>	<b>-3.92</b>	<b>-3.38</b>	<b>-3.97</b>	<b>-5.72</b>	<b>-6.88</b>	<b>-5.41</b>
Davis (-15)	<b>-1.28</b>	<b>-2.03</b>	-1.56	<b>-1.29</b>	<b>-1.61</b>	<b>-4.19</b>	<b>-5.98</b>	<b>-3.31</b>
Dumont Durville (+39)	<b>-0.53</b>	<b>-3.21</b>	<b>-3.56</b>	<b>-2.76</b>	-0.45	<b>-2.82</b>	<b>-4.07</b>	<b>-2.24</b>
Mawson (+205)	-0.28	<b>-2.62</b>	<b>-2.84</b>	<b>-2.53</b>	<b>-2.24</b>	<b>-4.32</b>	<b>-5.67</b>	<b>4.26</b>
McMurdo (+1)	<b>-3.45</b>	<b>-2.33</b>	<b>-3.12</b>	<b>-3.38</b>	<b>-7.13</b>	<b>-6.48</b>	<b>-8.11</b>	<b>-8.38</b>
Mirny (182)	<b>1.57</b>	-0.32	-0.01	0.08	<b>-1.24</b>	<b>-2.21</b>	<b>-2.97</b>	<b>-1.98</b>
Novolazarevskaya (+566)	0.38	<b>-2.33</b>	<b>-1.78</b>	<b>-1.33</b>	<b>2.49</b>	0.58	-1.02	0.58
Scott Base (+9)	<b>-1.36</b>	1	0.43	0.01	<b>-5.03</b>	<b>-3.15</b>	<b>-4.56</b>	<b>-4.98</b>
Syowa (+119)	<b>-2.31</b>	-0.53	-1.43	-0.75	-0.17	-0.58	<b>-1.49</b>	0.04
<i>Mean error</i>	-0.91	-1.76	-1.98	-1.70	-2.15	-3.34	-4.53	-3.33
<b>Ice shelves</b>	<b>ARP-AMIP-AC</b>				<b>ARP-AMIP</b>			
Halley (-17)	<b>2.68</b>	<b>6.84</b>	<b>7.54</b>	<b>5.38</b>	<b>1.27</b>	<b>2.45</b>	1.21	0.88
Neumayer (-58)	<b>3.21</b>	<b>5.45</b>	<b>6.58</b>	<b>5.25</b>	<b>2.18</b>	<b>1.21</b>	0.9	<b>1.41</b>
<i>Mean error</i>	.95	6.15	7.06	5.32	1.73	1.83	1.06	1.15
<b>Peninsula</b>	<b>ARP-AMIP-AC</b>				<b>ARP-AMIP</b>			
Bellingshausen (-2)	<b>-0.86</b>	0.3	0.11	0.08	<b>-1.02</b>	-0.42	-0.24	-0.08
Esperanza (+104)	<b>-1.66</b>	1.32	-0.76	-0.9	<b>-1.1</b>	0.5	-1.33	-0.88
Faraday (-10)	<b>-1.79</b>	<b>-1.23</b>	<b>-2.24</b>	<b>-2.12</b>	<b>-2.66</b>	<b>-4.66</b>	<b>-5.74</b>	<b>-3.66</b>
Marambio (-137)	<b>-2.34</b>	1.6	-1	-1.62	<b>-1.87</b>	1.04	-1.27	-1.6
Marsh (+4)	<b>-0.64</b>	0.36	0.06	0.13	<b>-0.81</b>	-0.36	-0.29	-0.03
Orcadas (-5)	<b>-0.92</b>	0.2	0.19	-0.64	<b>-1.13</b>	-0.04	0.61	-0.76
Rothera (+140)	<b>-2</b>	<b>-0.99</b>	<b>-3.14</b>	<b>-2.63</b>	<b>-5.55</b>	<b>-7.88</b>	<b>-8.72</b>	<b>-6.13</b>
<i>Mean error</i>	-1.46	0.22	-0.97	-1.1	-2.02	-1.69	-2.43	-1.88
<b>Southern Ocean</b>	<b>ARP-AMIP-AC</b>				<b>ARP-AMIP</b>			
Gough (-50)	<b>-1.05</b>	-0.3	0.12	<b>-0.71</b>	<b>-0.98</b>	-0.34	0.02	<b>-0.79</b>
Macquarie (-10)	<b>-0.47</b>	0.09	<b>0.39</b>	-0.25	<b>-0.71</b>	-0.35	0.2	<b>-0.45</b>
Marion (-17)	<b>-0.92</b>	<b>-0.43</b>	0.01	<b>-0.46</b>	<b>-1.15</b>	<b>-0.43</b>	-0.05	<b>-0.68</b>
<i>Mean error</i>	-0.81	-0.21	0.17	-0.47	-0.95	-0.37	0.06	-0.64

### Surface sublimation (mmWe yr<sup>-1</sup>), 1981-2010

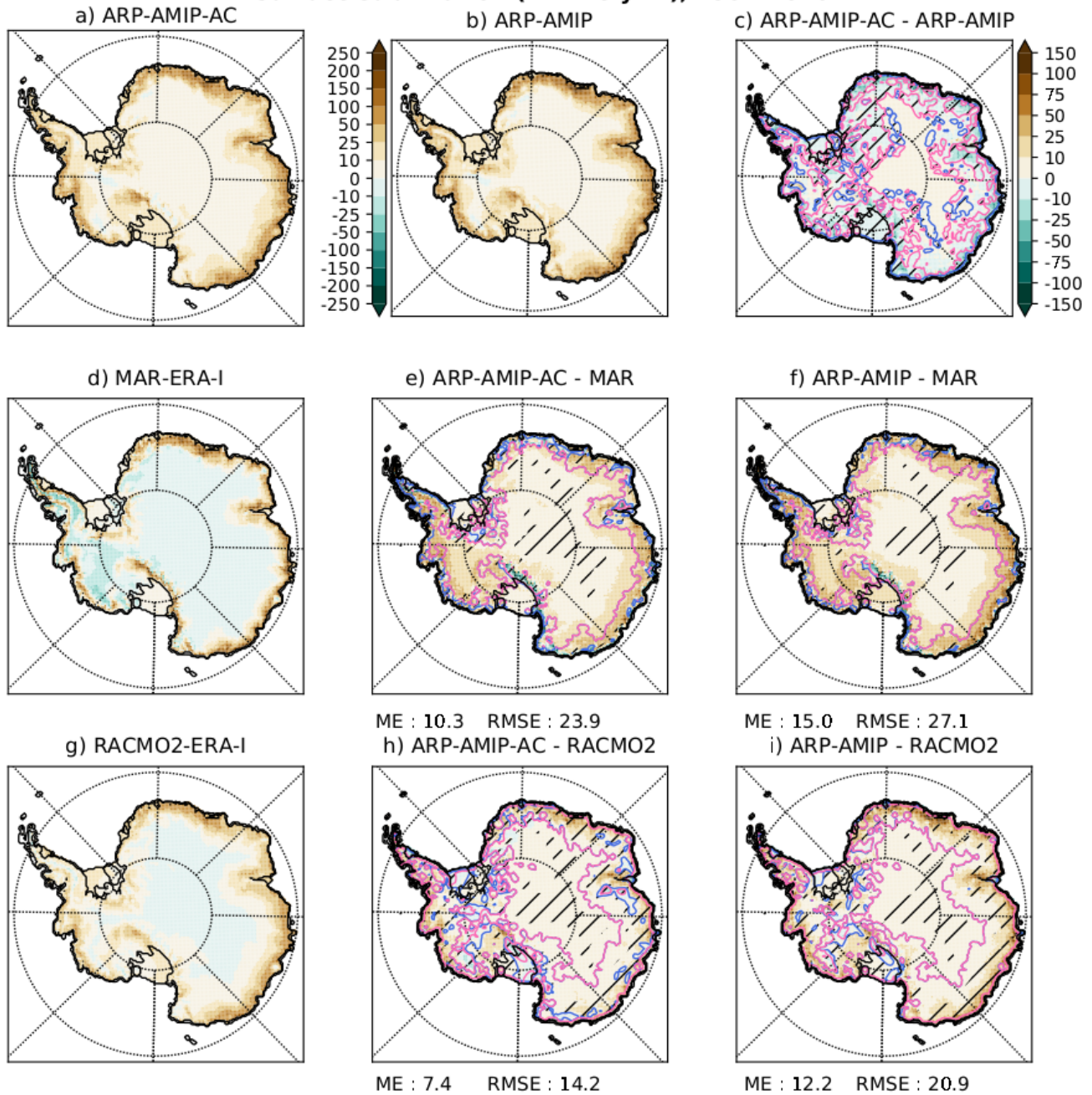


**Figure S9.** Yearly mean surface sublimation (mm w.e. yr<sup>-1</sup>) for ARP-AMIP-AC (a), ARP-AMIP (b), MAR-ERA-I (d) and RACMO-ERA-I (g) for the reference period 1981-2010. Difference (mm w.e. yr<sup>-1</sup>) for ARP-AMIP-AC minus ARP-AMIP (c), ARP-AMIP-AC minus MAR-ERA-I (e), ARP-AMIP minus MAR-ERA-I (f), ARP-AMIP-AC minus RACMO2-ERA-I (h) and ARP-AMIP minus RACMO2-ERA-I (i). Blue (magenta) hatched contour lines represent areas where the positive (negative) difference is larger than 20%. Mean error (ME) and RMSE statistics (mm w.e. yr<sup>-1</sup>) for the comparison with MAR and RACMO2 are shown below the subplot

## References

- Arblaster, J. M. and Meehl, G. A.: Contributions of External Forcings to Southern Annular Mode Trends, *Journal of Climate*, 19, 2896–2905, <https://doi.org/10.1175/JCLI3774.1>, 2006.
- Barnes, E. A. and Hartmann, D. L.: Detection of Rossby wave breaking and its response to shifts of the midlatitude jet with climate change, *Journal of Geophysical Research: Atmospheres*, 117, <https://doi.org/https://doi.org/10.1029/2012JD017469>, 2012.
- 5     Beaumont, J., Déqué, M., Krinner, G., Agosta, C., and Alias, A.: Effect of prescribed sea surface conditions on the modern and future Antarctic surface climate simulated by the ARPEGE atmosphere general circulation model, *The Cryosphere*, 13, 3023–3043, 2019.
- Bracegirdle, T. J., Shuckburgh, E., Sallee, J.-B., Wang, Z., Meijers, A. J. S., Bruneau, N., Phillips, T., and Wilcox, L. J.: Assessment of surface winds over the Atlantic, Indian, and Pacific Ocean sectors of the Southern Ocean in CMIP5 models: historical bias, forcing response, and state dependence, *Journal of Geophysical Research: Atmospheres*, 118, 547–562, <https://doi.org/10.1002/jgrd.50153>, 2013.
- 10    Bracegirdle, T. J., Hyder, P., and Holmes, C. R.: CMIP5 Diversity in Southern Westerly Jet Projections Related to Historical Sea Ice Area: Strong Link to Strengthening and Weak Link to Shift, *Journal of Climate*, 31, 195–211, <https://doi.org/10.1175/JCLI-D-17-0320.1>, 2018.
- Cesana, G., Waliser, D., Henderson, D., L'Ecuyer, T., Jiang, X., and Li, J.: The Vertical Structure of Radiative Heating Rates: A Multimodel Evaluation Using A-Train Satellite Observations, *Journal of Climate*, 32, 1573 – 1590, <https://doi.org/10.1175/JCLI-D-17-0136.1>, 2019.
- 15    Simpson, I. R., Blackburn, M., and Haigh, J. D.: A mechanism for the effect of tropospheric jet structure on the annular mode–like response to stratospheric forcing, *Journal of the atmospheric sciences*, 69, 2152–2170, 2012.
- Wilcox, L. J., Charlton-Perez, A. J., and Gray, L. J.: Trends in Austral jet position in ensembles of high- and low-top CMIP5 models, *Journal of Geophysical Research: Atmospheres*, 117, <https://doi.org/https://doi.org/10.1029/2012JD017597>, 2012.